

Frequency modulation of gravitational waves by ultralight scalar dark matter

Ke Wang^{1,2,3,*} and Yin Zhong^{2,3}

¹*Institute of Theoretical Physics & Research Center of Gravitation, Lanzhou University, Lanzhou 730000, China*

²*Key Laboratory of Quantum Theory and Applications of the Ministry of Education, Lanzhou University, Lanzhou 730000, China*

³*Lanzhou Center for Theoretical Physics & Key Laboratory of Theoretical Physics of Gansu Province, Lanzhou University, Lanzhou 730000, China*



(Received 19 June 2023; accepted 27 November 2023; published 18 December 2023)

The oscillating pressure of ultralight scalar dark matter (DM) can induce the oscillation of the local gravitational potential. Similarly to the time-dependent frequency shift for the pulse signals of pulsars, the oscillation of the local gravitational potential can induce a time-dependent frequency shift (or frequency modulation) for quasimonochromatic gravitational wave (GW) signals from Galactic white dwarf (WD) binaries. To make this effect detectable, we suppose that some Galactic WD binaries are located in DM clumps/subhalos where the energy density of DM is about 8 orders of magnitude higher than at the position of the Earth. Turning to the Fisher information matrix, we find that an amplified GW frequency modulation induced by ultralight scalar DM with a mass of $m = 1.67 \times 10^{-23} - 4.31 \times 10^{-23} \text{ eV}/c^2$ can be detected by LISA.

DOI: [10.1103/PhysRevD.108.123531](https://doi.org/10.1103/PhysRevD.108.123531)

I. INTRODUCTION

The rotational properties of galaxies [1], the evolution of large-scale structure [2], and gravitational lensing observations [3] are considered to be direct empirical proofs of the existence of dark matter (DM). Based on the standard Lambda-cold DM (Λ CDM) cosmological model, the latest cosmic microwave background (CMB) observations [4] further suggest that about 26% of the energy density in the Universe comes from CDM today. However, one of the most promising candidates for CDM—weak interacting massive particles (WIMPs) grounded on supersymmetric theories of particle physics—still has not been detected [5–8]. Moreover, primordial black holes which can also serve as CDM [9] still have not been identified. These null results, accompanied by CDM’s failure on subgalactic scales [10], imply that the standard CDM model may not be the final answer.

The de Broglie wavelength of the ultralight noninteracting particles with mass $\sim 10^{-22} \text{ eV}/c^2$ is comparable to astrophysical scales of $\sim 60 \text{ pc}$. As a result, ultralight particles can smooth out the inhomogeneities on small scales and prevent subgalactic structures from forming. According to this effect, an alternative candidate for DM is proposed. This ultralight DM (ULDM) not only can behave as CDM on large scales but also can avoid the CDM small-scale crises [11]. Also, due to its wave nature, the

pressure of ULDM is coherently oscillating. And the oscillation of the pressure can induce the oscillation of the metric in the DM halo. Similarly to gravitational waves (GWs), the time-dependent perturbations of the background metric induced by ULDM can also change the pulse arrival time of the pulsar and be detected by pulsar timing arrays (PTAs). The simplest cases, and the first to be investigated, are that ULDM consists of ultralight axion-like scalar particles [12–14]. After that, the pulsar timing residual induced by ultralight vector particles was investigated [15]. Recently, the pulsar timing residual induced by ultralight tensor particles has also been investigated [16].

Besides detecting ULDM with PTAs, many other detection methods of ULDM have been proposed. Similarly to GW detection, for example, the direct detection of ULDM wind by space-based laser interferometers such as the Laser Interferometer Space Antenna (LISA) [17] has been estimated [18]. ULDM can also affect the orbital motions of astrophysical objects in a galaxy and be detected indirectly [19,20]. Moreover, the black hole superradiant instability from ULDM can also constrain its mass [21].

In this paper, we propose a novel detection method of ULDM. Similarly to the time-dependent frequency shift for the pulse signals of pulsars, the oscillation of the local gravitational potential can induce a time-dependent frequency shift (or frequency modulation) for quasimonochromatic GW signals from Galactic white dwarf (WD) binaries. Although there are about 10^7 WD binaries in the Milky Way [22], the number of WD binaries with a chirp

*wangkey@lzu.edu.cn

mass measured by LISA is only about 1000 [23]. Here, we assume that some of the WD binaries with chirp mass measured by LISA are located in the DM clumps/subhalos.¹ The DM clumps/subhalos with mass $m \sim 10^7 M_\odot$ and size $r^3 \sim 10 \text{ pc}^3$ can serve as massive perturbors to explain many of the observed stream features in the GD-1 stellar stream, such as the spurs and the gaps [24,26]. As a result, the GW frequency modulation induced by the ultralight scalar DM will be amplified by about 8 orders of magnitude compared to the same effect taking place at the position of the Earth. Taking this mechanism into consideration and turning to the Fisher information matrix, we can estimate the detection of ultralight scalar DM by LISA [17].

This paper is organized as follows: In Sec. II, we estimate the detection of GW frequency modulation by LISA in a model-independent fashion. In Sec. III, we forecast the constraints on ultralight scalar DM imposed by the detection of GW frequency modulation. Finally, a brief summary and discussions are included in Sec. IV.

II. DETECTION OF GW FREQUENCY MODULATION BY LISA

A. GW signals and detector

Galactic WD binaries are supposed to be quasimonochromatic GW sources. Therefore, the GW signal from them in their own frame is defined as

$$h_+(t) = (\mathcal{A} + \delta\mathcal{A})(1 + \cos^2 \iota) \cos(\phi(t)), \quad (1)$$

$$h_\times(t) = -2(\mathcal{A} + \delta\mathcal{A}) \cos \iota \sin(\phi(t)), \quad (2)$$

where the involved derived parameters—including the dimensionless amplitude \mathcal{A} , the phase ϕ , the chirping frequency \dot{f}_0 , and the chirp mass \mathcal{M} —are defined as

$$\mathcal{A} = \frac{2(G\mathcal{M})^{5/3}(\pi f_0)^{2/3}}{c^4 d}, \quad (3)$$

$$\phi(t) = 2\pi f_0 t + \pi \dot{f}_0 (1 + \delta\dot{f}) t^2 + \phi_0, \quad (4)$$

¹On the one hand, the de Broglie wavelength of free ULDM with mass $\sim 10^{-22} \text{ eV}/c^2$ is much larger than the size of DM clumps/subhalos $r \sim 2 \text{ pc}$. On the other hand, the observations of the GD-1 stellar stream do favor such DM clumps/subhalos. We solve this tension by assuming that there is an additional local potential well $V(r) \approx \frac{1}{2} m \omega_0^2 r^2 + \dots$ at the location of the DM clump/subhalo. Then, the size of the DM clump/subhalo will be $r = \sqrt{\frac{\hbar}{m\omega_0}}$. And $r \sim 2 \text{ pc}$ just needs a very flat potential well with $\omega_0 \sim 10^{-10} \text{ Hz}$, where the behavior of ULDM will be very similar to that outside the DM clump/subhalo. Since such potential wells are formed coincidentally and the number of them is small (~ 100 [24]) in the Milky Way, their existence will not affect the statistical fact that ULDM suppresses the mass power spectrum on small scales [25].

TABLE I. Parameters of one specific WD binary and LISA constellation. The parameters in the first row are necessary to obtain the GW signal in the source frame. The parameters in the second row are necessary to obtain the GW response of the TDI observables. The parameters in the third row are newly introduced or derived parameters.

$m_1 [M_\odot]$	$m_2 [M_\odot]$	$d [\text{kpc}]$	$f_0 [\text{Hz}]$	$\iota [\text{rad}]$	$\phi_0 [\text{rad}]$
1	1	1	1×10^{-3}	$\frac{\pi}{4}$	0
$\psi [\text{rad}]$	$\beta [\text{rad}]$	$\lambda [\text{rad}]$	$L_i [\text{km}]$	$T [\text{yr}]$	e
$\frac{\pi}{4}$	$-\frac{\pi}{4}$	$\frac{\pi}{4}$	2.5×10^6	4	0.00964838
$\delta\mathcal{A}$	$\delta\dot{f}$	\mathcal{A}	$\dot{f}_0 [\text{Hz}^2]$	$\mathcal{M} [M_\odot]$	SNR
0	0	4.7×10^{-22}	4.6×10^{-18}	0.87	122

$$\dot{f}_0 = \frac{96}{5} \pi^{8/3} \left(\frac{G\mathcal{M}}{c^3} \right)^{5/3} f_0^{11/3}, \quad (5)$$

$$\mathcal{M} = \frac{(m_1 m_2)^{3/5}}{(m_1 + m_2)^{1/5}}. \quad (6)$$

The above derived parameters are further dependent on the primary and secondary WD masses m_1 and m_2 , the luminosity distance to the binary d , the frequency of GW f_0 , the orbital inclination ι , and the initial GW phase ϕ_0 . Besides these common parameters, we introduce two deviation parameters $\delta\mathcal{A}$ and $\delta\dot{f}$ to characterize the amplitude modulation and the frequency modulation during GW propagation. In the following discussion, we will consider a specific Galactic WD binary, whose parameters are listed in Table I.

Given that the three arm lengths of the LISA constellation [17] are $L_1 = L_2 = L_3 = 2.5 \times 10^6 \text{ km}$, the mission lifetime of the LISA is $T = 4 \text{ yr}$, and the eccentricity of the LISA spacecraft orbits in the Solar System barycentric ecliptic coordinate system is $e = 0.00964838$, we can calculate the GW response $h(t)$ of the second-generation time-delay interferometry (TDI) observables (e.g., X, Y, Z) for a GW source with polarization angle ψ at ecliptic latitude β and ecliptic longitude λ . Meanwhile, we can calculate the response of the second-generation TDI observables (e.g., X, Y, Z) to the combination of fundamental LISA noises including laser-frequency noise, proof-mass noise, and optical-path noise $n(t)$ or its power spectral density (PSD) $S_n(f)$. In this paper, we use Synthetic LISA [27] (C++/Python2.x) to simulate the response of the second-generation TDI observables (e.g., X, Y, Z) to GW signals and noises, as shown in Figs. 1 and 2, respectively. One can also use other simulators such as LISACode [28] or the analytical formulations [29–34] to obtain the GW and noise responses. Finally, the output of LISA is

$$s(t) = h(t) + n(t). \quad (7)$$

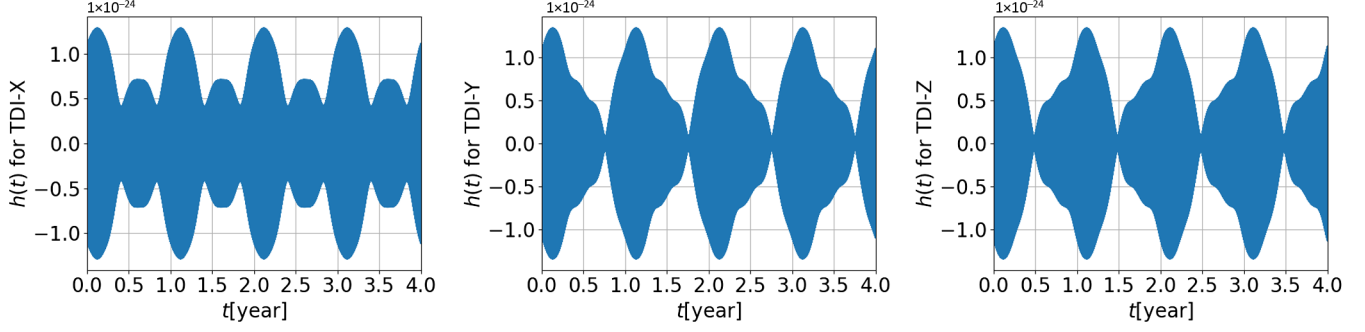


FIG. 1. The GW response of the second-generation TDI observables: X, Y, Z. The GW signal in the source frame is given by the parameters in the first row of Table I, and the detector's (LISA's) response is determined by the parameters in the second row of Table I.

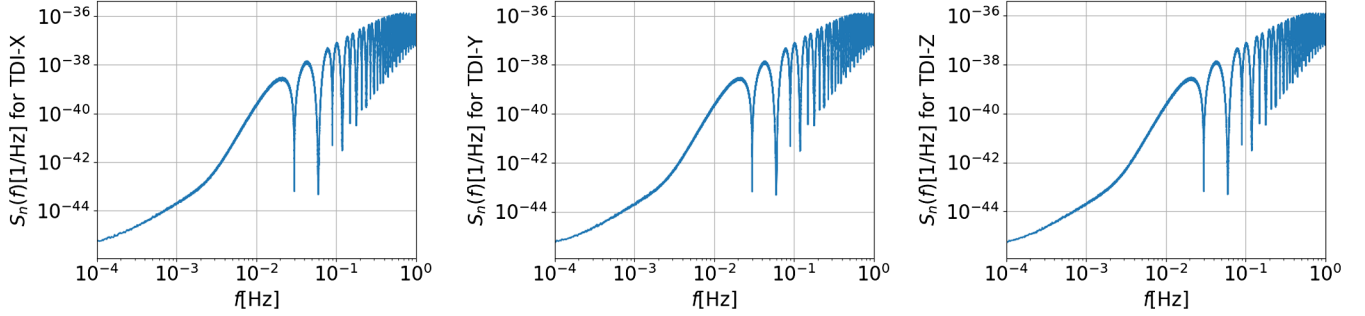


FIG. 2. The noise PSD derived from the response of the second-generation TDI observables X, Y, and Z to the combination of fundamental LISA noises: laser-frequency noise, proof-mass noise and optical-path noise, where $S_n(f_0) = 2.12 \times 10^{-44} \text{ Hz}^{-1}$, $S_n(f_0) = 2.07 \times 10^{-44} \text{ Hz}^{-1}$, and $S_n(f_0) = 2.01 \times 10^{-44} \text{ Hz}^{-1}$ for the X, Y, and Z channels, respectively.

To implement the parameter estimation, we should be able to tell $h(t)$ from $n(t)$. We can do that only for those sources whose signal-to-noise ratios (SNRs) are high enough:

$$\text{SNR}^2 = \sum_{X,Y,Z} 4\text{Re} \left(\int_0^\infty df \frac{\tilde{h}^*(f)\tilde{h}(f)}{S_n(f)} \right). \quad (8)$$

For quasimonochromatic GW sources with the initial frequency f_0 , we can use Parseval's theorem to rewrite SNR^2 in the time domain:

$$\text{SNR}^2 = \sum_{X,Y,Z} \frac{2}{S_n(f_0)} \int_0^T dt h(t)h(t). \quad (9)$$

In Table I, we also list the SNR for our example of a Galactic WD binary.

B. Fisher information matrix

To forecast the constraints on parameters, in this paper, we will turn to the Fisher information matrix:

$$\mathcal{F}_{ij} = \sum_{X,Y,Z} \frac{2}{S_n(f_0)} \int_0^T dt \frac{\partial h(t;\boldsymbol{\theta})}{\partial \theta_i} \frac{\partial h(t;\boldsymbol{\theta})}{\partial \theta_j}, \quad (10)$$

where $\boldsymbol{\theta}$ is a vector consisting of seven free parameters:

$$\boldsymbol{\theta} = \{\delta\mathcal{A}, \delta\dot{f}, \iota, \phi_0, \psi, \beta, \lambda\}.$$

The root mean square errors of these parameters are given by

$$\sigma_i = \sqrt{(\mathcal{F}^{-1})_{ii}}. \quad (11)$$

To numerically plug the GW responses of TDI observables $h(t;\boldsymbol{\theta})$ and the noise PSD $S_n(f)$ into Eq. (10), we rewrite the Fisher information matrix calculation package for GW detector networks, GWFISH [35] (Python3.x) in Python2.x, and make it compatible with Synthetic LISA [27] (C++/Python2.x). Finally, we use GWFISH to obtain the measurement uncertainties, as listed in Table II. In this paper, we only care

TABLE II. Measurement uncertainties obtained with Synthetic LISA plugged into GWFISH. The errors are at a 68% confidence level.

$\delta\mathcal{A}$	$\delta\dot{f}$	ι [rad]	ϕ_0 [rad]
0 ± 0.041	0 ± 0.098	$\frac{\pi}{4} \pm 0.049$	$\frac{\pi}{4} \pm 0.14$
ψ [rad]	β [rad]	λ [rad]	
$\frac{\pi}{4} \pm 0.070$	$-\frac{\pi}{4} \pm 0.0053$	$\frac{\pi}{4} \pm 0.0057$	

about $\sigma_{\delta\dot{f}}$, which is the error of $\delta\dot{f}$. From the definition of $\delta\dot{f}$, we know that frequency modulations during GW propagation larger than $\sigma_{\delta\dot{f}}\dot{f} = 4.5 \times 10^{-19} \text{ Hz}^2$ will be detected by LISA.

III. FORECASTING THE CONSTRAINTS ON ULTRALIGHT SCALAR DM

If we confirm that GW signals are quasimonochromatic in their source frame, they can be considered to be a unique probe during GW propagation. For example, the amplitude modulation taking place during GW propagation implies that there may be an evolving gravitational lens [36]. In this paper, we will investigate the frequency modulation induced by ultralight scalar DM during GW propagation.

Since the pressure of ultralight scalar DM is coherently oscillating in the Galactic, the surrounding metric has the following form:

$$ds^2 = (1 + 2\Phi(\mathbf{x}, t))^2 dt^2 - (1 - 2\Psi(\mathbf{x}, t))\delta_{ij}dx^i dx^j, \quad (12)$$

where the induced gravitational potentials $\Psi(\mathbf{x}, t)$ can be decomposed into the time-independent part $\Psi_c(\mathbf{x})$ and the oscillating part $\Psi_o(\mathbf{x}) \cos(\omega t + 2\alpha(\mathbf{x}))$. Given the mass m , the local energy density $\rho(\mathbf{x})$, and the local velocity $v(\mathbf{x})$ of DM particles, the two parts of $\Psi(\mathbf{x}, t)$ can be obtained from Einstein equations [12]:

$$\begin{aligned} \Psi_o(\mathbf{x}) &= \frac{\pi\hbar^2 G\rho(\mathbf{x})}{m^2 c^6} \\ &= 6.48 \times 10^{-16} \left(\frac{\rho(\mathbf{x})}{0.4 \text{ GeV/cm}^3} \right) \left(\frac{10^{-23} \text{ eV}}{mc^2} \right)^2, \end{aligned} \quad (13)$$

$$\Psi_c(\mathbf{x}) = \frac{4\pi\hbar^2 G\rho(\mathbf{x})}{m^2 c^4 v^2(\mathbf{x})} = 4 \times 10^6 \left(\frac{10^{-6} c^2}{v^2(\mathbf{x})} \right) \Psi_o(\mathbf{x}), \quad (14)$$

$$\omega = \frac{2mc^2}{\hbar} = 3 \times 10^{-8} \text{ Hz} \left(\frac{mc^2}{10^{-23} \text{ eV}} \right). \quad (15)$$

Therefore, a signal propagating in this metric will suffer a frequency shift

$$f_e - f_s = f_s(\Psi(\mathbf{x}_e, t_e) - \Psi(\mathbf{x}_s, t_s)), \quad (16)$$

where the observables with the subscript e are the ones detected at the Earth, and the observables with the subscript s are the ones detected at the source. That is to say, this signal will suffer a frequency redshift $f_e < f_s$ when $\Psi(\mathbf{x}_e, t_e) < \Psi(\mathbf{x}_s, t_s)$. At the position of the Earth, the velocity of DM is $v(\mathbf{x}_e) \sim 10^{-3}c$, and the energy density of DM is $\rho(\mathbf{x}_e) = 0.4 \text{ GeV/cm}^3$ [37]. For a very nearby signal source [$d \sim 100 \text{ pc}$, $\Psi_o(\mathbf{x}_e) \approx \Psi_o(\mathbf{x}_s)$ and

$\Psi_c(\mathbf{x}_e) \approx \Psi_c(\mathbf{x}_s)$], ultralight scalar DM with mass $m = 10^{-23} \text{ eV}/c^2$ can induce a frequency shift $f_e - f_s \sim 10^{-16}f_s$ in years. This tiny novel effect on the pulse frequency of the pulsar can be accumulated, and it changes the pulse arrival time of the pulsar [12], and then it can be detected by the pulsar timing arrays [14].

If one wants this simple frequency shift effect on the quasimonochromatic GW signals from Galactic WD binaries to be detected by LISA, the GW sources should be located in some DM clumps/subhalos [24,26], where the energy density of DM is allowed to be $\rho(\mathbf{x}_s) \approx \frac{10^7 M_\odot c^2}{10 \text{ pc}^3} \approx 10^8 \rho(\mathbf{x}_e)$. In this paper, we will consider ultralight scalar DM with mass $m = n \times 10^{-23} \text{ eV}/c^2$, velocity $v(\mathbf{x}_s) = 1 \times 10^{-3}c$, and phase $\alpha(\mathbf{x}_s) = 0$. Then, we have $\Psi_o(\mathbf{x}_s) = 10^8 \Psi_o(\mathbf{x}_e) = \frac{6.48}{n^2} \times 10^{-8}$, $\Psi_c(\mathbf{x}_s) = 10^8 \Psi_c(\mathbf{x}_e) = \frac{2.59}{n^2} \times 10^{-1}$, and $\omega = 3n \times 10^{-8} \text{ Hz}$. Then, a GW signal with $f_s = f_0 = 1 \times 10^3 \text{ Hz}$ from such a DM clump suffers a frequency redshift

$$f_e - f_0 = -f_0(\Psi_c(\mathbf{x}_s) + \Psi_o(\mathbf{x}_s) \cos(\omega t)). \quad (17)$$

The first part, $-f_0 \Psi_c(\mathbf{x}_s) = -\frac{2.59}{n^2} \times 10^{-4} \text{ Hz}$, is a time-independent frequency redshift. For $n > 1$, it is not only negligible compared to $f_0 = 1 \times 10^3 \text{ Hz}$, but also degenerate with \mathcal{A} , \mathcal{M} , and d , as shown in Eq. (3). The second part, $-f_0 \Psi_o(\mathbf{x}_s) \cos(\omega t) = -\frac{6.48}{n^2} \times 10^{-11} \cos(\omega t) \text{ Hz}$, is a time-dependent frequency modulation with $\dot{f}_e = \frac{1.94}{n} \times 10^{-18} \sin(\omega t) \text{ Hz}^2$. On the one hand, the detection of at least one oscillation of ultralight scalar DM during LISA's mission lifetime $T = 4 \text{ yr}$ requires that ω be larger than $5 \times 10^{-8} \text{ Hz}$ and that n be larger than 1.67; on the other hand, $\dot{f}_e > \sigma_{\delta\dot{f}}\dot{f}_0$ requires that n be smaller than 4.31. That is to say, LISA can detect ultralight scalar DM with mass $m = 1.67 \times 10^{-23} - 4.31 \times 10^{-23} \text{ eV}/c^2$ through the frequency modulation of quasimonochromatic GW from Galactic WD binaries located in DM clumps/subhalos.

In Fig. 3, the evolution of \dot{f}_e only due to the GW radiation is the blue solid line, which just changes by 0.001% during LISA's mission lifetime. The evolution of \dot{f}_e due to the GW radiation and the frequency modulation by ultralight scalar DM with mass $m = 1.94 \times 10^{-23} \text{ eV}/c^2$ is the blue dotted curve, which is oscillating across the measurement uncertainty of \dot{f}_e (blue dashed lines). These oscillating features are very distinguishable from the other simple chirping signals. For example, as GW radiation drives the components of a Galactic WD binary closer together, the effects of mass transfer and tidal forces will dominate the evolution of a negative \dot{f}_e in 10^5 yr [38]. The peculiar acceleration caused by a variation of the center-of-mass velocity of a Galactic WD binary will obtain a Doppler-shifted \dot{f}_e [39].

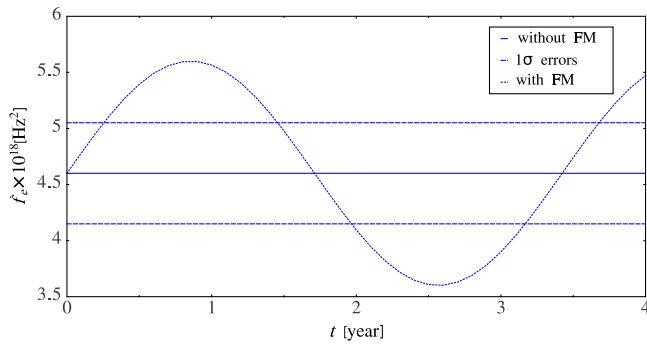


FIG. 3. The evolution of f_e during LISA's mission lifetime. Without the frequency modulation by ultralight scalar DM, f_e just changes by 0.001% during LISA's mission lifetime (blue solid line), and the measurement uncertainty of f_e is given by $f_e(1 \pm \sigma_{\delta f})$ (blue dashed lines). Taking the frequency modulation by ultralight scalar DM with mass $m = 1.94 \times 10^{-23}$ eV/ c^2 into consideration, the evolution of f_e is oscillating during LISA's mission lifetime (blue dotted curve).

IV. SUMMARY AND DISCUSSION

In this paper, inspired by the time-dependent frequency shift for the pulse signals of pulsars due to the oscillating pressure of the ultralight scalar DM, we propose a novel detection method of the ultralight scalar DM. Similarly to the pulse signals of pulsars, the quasimonochromatic GW signals from Galactic WD binaries can also be considered as a probe to gather the oscillation information of the ultralight scalar DM during GW propagation. For $\rho(\mathbf{x}_s) \approx \rho(\mathbf{x}_e) = 0.4$ GeV/cm³ [37], the time-dependent frequency shift for the pulse signals of pulsars can be accumulated in the arrival time of pulses, but the time-dependent frequency shift for the quasimonochromatic GW signals from Galactic WD binaries is very tiny. If we suppose that some WD binaries are located in the DM clumps/subhalos where $\rho(\mathbf{x}_s) \approx \frac{10^7 M_\odot c^2}{10 \text{ pc}^3} \approx 10^8 \rho(\mathbf{x}_e)$, the time-dependent frequency

shift for the quasimonochromatic GW signals from Galactic WD binaries will be amplified accordingly. Compared to $\sigma_{\delta f}$ estimated by the Fisher information matrix, the frequency modulation of quasimonochromatic GW from Galactic WD binaries located in DM clumps/subhalos induced by the ultralight scalar DM with mass $m = 1.67 \times 10^{-23} - 4.31 \times 10^{-23}$ eV/ c^2 will be detected by LISA.

There are two caveats. The first one is that we have supposed that some Galactic WD binaries with chirp mass measured by LISA are located in the DM clumps/subhalos. Given the number of such WD binaries (about 1000) and the number of DM clumps/subhalos (about 100) in the Milky Way, this assumption seem to be reasonable. But in reality, we do not know the true distribution of WD binaries in the Milky Way. We also do not know whether or not the WD binaries are excluded from the DM clumps/subhalos. The second one is the conflict between the concept of ULDM and the concept of DM clumps/subhalos. The former is introduced to suppress the subgalactic structures, but the latter is just the subgalactic structure. We do not know how ULDM forms the DM clumps/subhalos. Here, we just assume that there is an additional local potential well at the location of DM clumps/subhalos. All in all, the detection of GW frequency modulation can also help us to investigate the DM clumps/subhalos in the Milky Way.

ACKNOWLEDGMENTS

We acknowledge the use of the HPC Cluster of Tianhe II in National Supercomputing Center in Guangzhou. K.W. is supported by grants from the National Key Research and Development Program of China (Grant No. 2021YFC2203003), grants from NSFC (Grants No. 12005084 and No. 12247101), and grants from the China Manned Space Project with Grant No. CMS-CSST-2021-B01.

-
- [1] V. C. Rubin, W. K. Ford, Jr., N. Thonnard, and D. Burstein, Rotational properties of 23 SB galaxies, *Astrophys. J.* **261**, 439 (1982).
 - [2] M. Davis, G. Efstathiou, C. S. Frenk, and S. D. M. White, The evolution of large scale structure in a universe dominated by cold dark matter, *Astrophys. J.* **292**, 371 (1985).
 - [3] D. Clowe, M. Bradac, A. H. Gonzalez, M. Markevitch, S. W. Randall, C. Jones, and D. Zaritsky, A direct empirical proof of the existence of dark matter, *Astrophys. J. Lett.* **648**, L109 (2006).
 - [4] N. Aghanim *et al.* (Planck Collaboration), Planck 2018 results: VI. Cosmological parameters, *Astron. Astrophys.* **641**, A6 (2020); **652**, C4(E) (2021).
 - [5] A. Tan *et al.* (PandaX-II Collaboration), Dark matter results from first 98.7 days of data from the PandaX-II experiment, *Phys. Rev. Lett.* **117**, 121303 (2016).
 - [6] D. S. Akerib *et al.* (LUX Collaboration), Improved limits on scattering of weakly interacting massive particles from reanalysis of 2013 LUX data, *Phys. Rev. Lett.* **116**, 161301 (2016).

- [7] L. Accardo *et al.* (AMS Collaboration), High statistics measurement of the positron fraction in primary cosmic rays of 0.5–500 GeV with the alpha magnetic spectrometer on the international space station, *Phys. Rev. Lett.* **113**, 121101 (2014).
- [8] M. Ackermann *et al.* (Fermi-LAT Collaboration), Measurement of separate cosmic-ray electron and positron spectra with the Fermi Large Area Telescope, *Phys. Rev. Lett.* **108**, 011103 (2012).
- [9] B. Carr, F. Kuhnel, and M. Sandstad, Primordial black holes as dark matter, *Phys. Rev. D* **94**, 083504 (2016).
- [10] J. Primack, Cosmology: Small scale issues revisited, *New J. Phys.* **11**, 105029 (2009).
- [11] W. Hu, R. Barkana, and A. Gruzinov, Cold and fuzzy dark matter, *Phys. Rev. Lett.* **85**, 1158 (2000).
- [12] A. Khmelnitsky and V. Rubakov, Pulsar timing signal from ultralight scalar dark matter, *J. Cosmol. Astropart. Phys.* **02** (2014) 019.
- [13] D. J. E. Marsh, Axion cosmology, *Phys. Rep.* **643**, 1 (2016).
- [14] R. Kato and J. Soda, Search for ultralight scalar dark matter with NANOGrav pulsar timing arrays, *J. Cosmol. Astropart. Phys.* **09** (2020) 036.
- [15] K. Nomura, A. Ito, and J. Soda, Pulsar timing residual induced by ultralight vector dark matter, *Eur. Phys. J. C* **80**, 419 (2020).
- [16] Y. M. Wu, Z. C. Chen, and Q. G. Huang, Pulsar timing residual induced by ultralight tensor dark matter, *J. Cosmol. Astropart. Phys.* **09** (2023) 021.
- [17] P. Amaro-Seoane *et al.* (LISA Collaboration), Laser interferometer space antenna, [arXiv:1702.00786](https://arxiv.org/abs/1702.00786).
- [18] A. Aoki and J. Soda, Detecting ultralight axion dark matter wind with laser interferometers, *Int. J. Mod. Phys. D* **26**, 1750063 (2016).
- [19] D. Blas, D. L. Nacir, and S. Sibiryakov, Ultralight dark matter resonates with binary pulsars, *Phys. Rev. Lett.* **118**, 261102 (2017).
- [20] M. Bošković, F. Duque, M. C. Ferreira, F. S. Miguel, and V. Cardoso, Motion in time-periodic backgrounds with applications to ultralight dark matter haloes at galactic centers, *Phys. Rev. D* **98**, 024037 (2018).
- [21] R. Brito, S. Grillo, and P. Pani, Black hole superradiant instability from ultralight spin-2 fields, *Phys. Rev. Lett.* **124**, 211101 (2020).
- [22] G. Nelemans, L. R. Yungelson, and S. F. Portegies Zwart, The gravitational wave signal from the galactic disk population of binaries containing two compact objects, *Astron. Astrophys.* **375**, 890 (2001).
- [23] A. Lamberts, S. Blunt, T. B. Littenberg, S. Garrison-Kimmel, T. Kupfer, and R. E. Sanderson, Predicting the LISA white dwarf binary population in the Milky Way with cosmological simulations, *Mon. Not. R. Astron. Soc.* **490**, 5888 (2019).
- [24] N. Mirabal and A. Bonaca, Machine-learned dark matter subhalo candidates in the 4FGL-DR2: Search for the perturber of the GD-1 stream, *J. Cosmol. Astropart. Phys.* **11** (2021) 033.
- [25] L. Hui, Wave dark matter, *Annu. Rev. Astron. Astrophys.* **59**, 247 (2021).
- [26] A. Bonaca, D. W. Hogg, A. M. Price-Whelan, and C. Conroy, The spur and the gap in GD-1: Dynamical evidence for a dark substructure in the Milky Way halo, [arXiv:1811.03631](https://arxiv.org/abs/1811.03631).
- [27] M. Vallisneri, Synthetic LISA: Simulating time delay interferometry in a model LISA, *Phys. Rev. D* **71**, 022001 (2005).
- [28] A. Petiteau, G. Auger, H. Halloin, O. Jeannin, E. Plagnol, S. Pireaux, T. Regimbau, and J. Y. Vinet, LISACode: A scientific simulator of LISA, *Phys. Rev. D* **77**, 023002 (2008).
- [29] C. Cutler, Angular resolution of the LISA gravitational wave detector, *Phys. Rev. D* **57**, 7089 (1998).
- [30] F. B. Estabrook, M. Tinto, and J. W. Armstrong, Time delay analysis of LISA gravitational wave data: Elimination of spacecraft motion effects, *Phys. Rev. D* **62**, 042002 (2000).
- [31] N. J. Cornish and L. J. Rubbo, The LISA response function, *Phys. Rev. D* **67**, 022001 (2003); **67**, 029905(E) (2003).
- [32] T. A. Prince, M. Tinto, S. L. Larson, and J. W. Armstrong, The LISA optimal sensitivity, *Phys. Rev. D* **66**, 122002 (2002).
- [33] T. Robson, N. J. Cornish, and C. Liu, The construction and use of LISA sensitivity curves, *Classical Quantum Gravity* **36**, 105011 (2019).
- [34] S. Babak, A. Petiteau, and M. Hewitson, LISA sensitivity and SNR calculations, [arXiv:2108.01167](https://arxiv.org/abs/2108.01167).
- [35] U. Dupletsa, J. Harms, B. Banerjee, M. Branchesi, B. Goncharov, A. Maselli, A. C. S. Oliveira, S. Ronchini, and J. Tissino, GWFISH: A simulation software to evaluate parameter-estimation capabilities of gravitational-wave detector networks, *Astron. Comput.* **42**, 100671 (2023).
- [36] Y. Qiu, K. Wang, and J. h. He, Amplitude modulation in binary gravitational lensing of gravitational waves, [arXiv:2205.01682](https://arxiv.org/abs/2205.01682).
- [37] F. Nesti and P. Salucci, The dark matter halo of the Milky Way, AD 2013, *J. Cosmol. Astropart. Phys.* **07** (2013) 016.
- [38] K. Kremer, K. Breivik, S. L. Larson, and V. Kalogera, Accreting double white dwarf binaries: Implications for LISA, *Astrophys. J.* **846**, 95 (2017).
- [39] Z. Xuan, P. Peng, and X. Chen, Degeneracy between mass and peculiar acceleration for the double white dwarfs in the LISA band, *Mon. Not. R. Astron. Soc.* **502**, 4199 (2021).